© 2021. Published by The Company of Biologists Ltd | Journal of Cell Science (2021) 134, jcs252528. doi:10.1242/jcs.252528

RESEARCH ARTICLE

SPECIAL ISSUE: CELL BIOLOGY OF HOST–PATHOGEN INTERACTIONS

Neonatal low-density granulocytes internalize and kill bacteria but suppress monocyte function using extracellular DNA

Brittany G. Seman[1], Jordan K. Vance[1], Stephen M. Akers[2] and Cory M. Robinson[1,3,*]

ABSTRACT

Low-density granulocytes (LDGs) are found abundantly in neonatal blood; however, there is limited mechanistic understanding of LDG interactions with bacteria and innate immune cells during acute infection. We aimed to determine how human neonatal LDGs may influence control of the bacterial burden at sites of infection, both individually and in the presence of mononuclear phagocytes. LDGs from human umbilical cord blood do phagocytose *Escherichia coli* O1:K1:H7 and traffic bacteria into acidic compartments. However, LDGs were significantly less efficient at bacterial uptake and killing compared to monocytes, and this activity was associated with a reduced inflammatory cytokine response. The presence of bacteria triggered the release of DNA (eDNA) from LDGs into the extracellular space that resembled neutrophil extracellular traps, but had limited anti-bacterial activity. Instead, eDNA significantly impaired monocyte control of bacteria during co-culture. These results suggest that LDG recruitment to sites of bacterial infection may compromise host protection in the neonate. Furthermore, our findings reveal novel insights into LDG activity during infection, clarify their inflammatory contributions relative to monocytes, and identify a novel LDG mechanism of immunosuppression.

This article has an associated First Person interview with the first author of the paper.

KEY WORDS: Low-density granulocyte, Extracellular DNA, Innate immunity, MDSC, Neutrophil, Neonatal

INTRODUCTION

Neonatal immune biology reflects a distinct, regulatory state compared to that in adults. Consistent with this observation, neonates are more susceptible to microbial pathogens and suffer disproportionately from infectious diseases (Weston et al., 2011). Although there are increases in T cells, B cells, neutrophils and monocytes in neonates compared to adults (Sharma et al., 2012), differences in activity and function relative to adult counterparts most likely contribute to the host susceptibility to infection (Simon et al., 2015). Understanding mechanistic explanations for limitations in neonatal immunity is paramount to development of host-directed interventions that can improve outcomes in this vulnerable population.

[1]Department of Microbiology, Immunology, & Cell Biology, West Virginia University School of Medicine, Morgantown, WV 26506, USA. [2]Department of Pediatrics, West Virginia University School of Medicine, Morgantown, WV 26506, USA. [3]Vaccine Development Center at West Virginia University Health Sciences Center, Morgantown, WV 26506, USA.

*Author for correspondence (cory.robinson1@hsc.wvu.edu)

B.G.S., 0000-0003-0660-1723; S.M.A., 0000-0002-3810-9656; C.M.R., 0000-0002-2122-2046

Handling Editor: Daniel Billadeau
Received 31 July 2020; Accepted 1 February 2021

An important distinction in the neonatal immune profile is the abundance of low-density granulocytes (LDGs) that resemble neutrophils and reside in the mononuclear cell fraction during density gradient centrifugation (Scapini et al., 2016; Carmona-Rivera and Kaplan, 2013). These cells are considered separate from normal-density neutrophils (NDNs), and have been shown to expand as a population during certain pathological conditions, including infection (Ui Mhaonaigh et al., 2019; Nicolás-Ávila et al., 2017; La Manna et al., 2019). LDGs have been referred to as low-density neutrophils (LDNs) and granulocytic myeloid-derived suppressor cells (gMDSCs), and have been ascribed a range of suppressive activity toward T cells, depending on the report (Köstlin et al., 2014; Leiber et al., 2017; Bowers et al., 2014; Alfaro et al., 2016). Whether LDNs and gMDSCs are interchangeable descriptions or definitive cell populations remains to be established. Other complexities that surround this possibility are potential changes in abundance, activity or suppressive state amongst different individuals and with accompanying disease states. Additional questions surround the activity level of LDGs specifically isolated from neonatal blood, and how they may further contribute to the early-life immune response and susceptibility to infection. Moreover, there are currently no studies that have adequately addressed the response of neonatal LDGs to bacteria commonly responsible for acute neonatal infections.

LDGs have important immune suppressive functions during disease, but these can vary depending on whether they are defined as LDNs or gMDSCs. Originally, gMDSCs were observed to promote cancer progression by suppressing anti-tumor immunity and compromising T cell surveillance (Young et al., 1987; Bronte et al., 2000). A general population of MDSCs also suppress natural killer (NK) cell production of interferon γ (IFNγ) through cell-to-cell contact, and transforming growth factor β (TGF-β) production (Li et al., 2009). MDSCs and LDNs have both been reported to express a multitude of proinflammatory and anti-inflammatory cytokines, including tumor necrosis factor α (TNF-α, also known as TNF) and interleukin-10 (IL-10) (Janols et al., 2014; Poe et al., 2013; Denny et al., 2010). Our lab has recently determined murine MDSCs to be a source of IL-27, a pleiotropic cytokine known to suppress inflammation (Gleave Parson et al., 2019). Taken together, this body of literature suggests that LDGs are not only abundant in the neonatal immune system, but they may be important regulators of immunity in early life.

LDGs have been implicated in the altered function of other immune cell populations during infection. Our lab has demonstrated that murine macrophages are impaired in their ability to clear bacteria *in vitro* in the presence of MDSCs (Gleave Parson et al., 2019). Monocytes from human umbilical cord blood are also impaired in their ability to stimulate T cell activation and express lower levels of heterodimeric integrins involved in phagocytosis in the presence of MDSCs (Dietz et al., 2019). MDSCs have been involved in the immune shift towards an anti-inflammatory state

Journal of Cell Science (2021) 134, jcs252528. doi:10.1242/jcs.252528

during late-onset sepsis induced by cecal ligation and puncture in mice (Brudecki et al., 2012). However, few studies have investigated the direct interactions that occur between LDGs and microbes, or how these interactions contribute to the complete immune response during infection. Although gMDSCs and LDGs share a common progenitor with professional phagocytes, their phagocytic capabilities have yet to be fully analyzed. Murine gMDSCs have been shown to have the potential to phagocytose latex beads (Youn et al., 2012). Davis and colleagues briefly suggest that MDSCs can phagocytose *Escherichia coli* particles *in vitro* (Davis et al., 2017); however, the mechanistic details were not analyzed in depth, nor were 3D reconstructive analyses utilized to determine whether bacteria were internalized in the cells. In other reports, LDNs have been described to have a decreased or absent capacity for phagocytosis of pHrodo-labeled *Staphylococcus aureus* particles and *Mycobacterium tuberculosis* compared to that of NDNs, although again, mechanistic details were not fully analyzed in depth (La Manna et al., 2019; Denny et al., 2010). As such, our mechanistic understanding of direct LDG interactions with bacterial pathogens, the fate of the bacteria and the net contribution during infection has remained limited.

In this report, we describe the interactions of LDGs obtained from umbilical cord blood with bacteria and monocytes during *in vitro* infection. The major objective was to understand how LDGs regulate control of the bacterial burden in this infection model. This required measuring bacterial uptake and killing for each cell type comparatively, as well as in co-culture. Separate studies have compared LDN and NDN activity, but this is the first study to compare LDG antibacterial activity with that of mononuclear cells in the same fraction of blood and provide novel insights. We examined the capacity of LDGs and monocytes to phagocytose *E. coli* serotype O1:K1:H7 through 3D time-lapse microscopy, flow cytometry and bacterial killing assays. This serotype is a leading cause of invasive neonatal infections, such as sepsis and meningitis, and is responsible for significant mortality (Simonsen et al., 2014; Stoll et al., 2011). Our data demonstrate several new mechanistic insights into LDG biology. Although LDGs are capable of phagocytic uptake and elimination of bacteria, they are functionally limited compared to professional mononuclear phagocytes. Additionally, we found that neonatal LDGs release DNA into the extracellular environment, although this function is not associated with potent bactericidal activity. In contrast, bacterial clearance by monocytes co-cultured with LDGs is significantly improved in the absence of extracellular DNA. Lastly, LDGs from healthy neonates in our study do not possess the potent suppression of T cell proliferation that is traditionally associated with classical MDSCs. However, they do compromise an effective innate immune response during bacterial infection, demonstrating suppression in a different way. Overall, this study demonstrates novel LDG functionality, and gives rise to new considerations for LDGs in the complete host response during acute infections. Our study further challenges the paradigm for how to define these cells, and we propose a spectrum of neutrophil activity that may arise in response to varying host conditions.

RESULTS

LDGs are less efficient at bacterial killing compared to monocytes

Our understanding of how LDGs and monocytes may interact at sites of bacterial infection is incomplete. It is also unclear whether the abundant LDGs in human neonatal blood universally have MDSC-like activity, functionally defined by the ability to limit T cell proliferation (Ostrand-Rosenberg et al., 2012; Chen et al., 2017). Using density gradient separation, we isolated $CD66^+$ cells from the low-density fraction by immunomagnetic selection. Our isolation strategy is analogous to other studies that have analyzed gMDSCs (Rieber et al., 2013a,b; Dumitru et al., 2012; Cassetta et al., 2019; Bronte et al., 2016; Leiber et al., 2017). Based on immunolabeling and flow cytometry, this LDG population was $CD66^{hi}$, $CD33^+$, $CD14^{lo}$ and $HLA\text{-}DR^-$ (Fig. S1A,B). At equal ratios, the neonatal LDGs mildly suppressed $CD4^+$ and $CD8^+$ T cell proliferation induced by IL-2 and CD3/CD28 stimulation (Fig. S2). Although there is no formal numerical criteria that we are aware of, it is our belief that an approximate 25% T cell reduction would not broadly be considered a classical MDSC level of expression. For the purposes of clarity in this report, we refer to these cells that stain as LDGs. Different names have been ascribed to this population in the literature, including LDG, LDN and gMDSC, and reflects the ongoing efforts to further characterize this cell population. When reference is made to other published reports, we will use the names utilized by the authors of those reports to respect their original intent.

In human blood, LDGs separate in the same fraction as mononuclear cells following density gradient centrifugation. Before determining how LDGs influence bacterial killing during co-culture with monocytes, it was first important to characterize the individual contributions of each cell type. Significantly less is known about how LDGs interact directly with bacterial pathogens. To determine whether LDGs are able to eliminate bacteria at all or at a level comparable to primary monocytes, we implemented a previously described gentamicin protection assay (Gleave Parson et al., 2019). Briefly, LDGs or monocytes were infected with *E. coli* O1:K1:H7 for 1 h, and then treated with gentamicin to kill extracellular bacteria. Following 2 h of gentamicin exposure, LDGs and monocytes were permeabilized with 1% saponin at varying time points to quantify bacterial recovery. Previous work in our lab has shown that following 2 h of gentamicin treatment, extracellular bacteria are non-viable (Gleave Parson et al., 2019). To account for any differences in bacterial uptake between cell types, killing efficiency at later time points was normalized to bacteria present within the intracellular compartment of each cell type at 2 h. We found a significantly higher bacterial recovery from LDGs at 6 and 18 h post gentamicin exposure (Fig. 1). However, by 24 h, bacterial recovery from LDGs was comparable to that from monocytes (Fig. 1). Overall, these results suggest that although LDGs are capable of bacterial elimination, they are significantly less efficient at this function relative to monocytes.

LDGs are less efficient at phagocytosis of bacteria relative to monocytes

LDGs are able to kill bacteria during infection, but at a significantly slower rate compared to monocytes. Although killing efficiency was normalized to bacterial uptake at 2 h for each cell type, it was apparent that there were important differences in bacterial internalization. As such, we wanted to determine the kinetics and efficiency of LDG phagocytosis of bacteria compared to that by monocytes. To determine the ability of LDGs to eliminate bacteria upon phagocytosis, we infected cells with fluorescently-labeled *E. coli* and longitudinally quantified uptake and bacterial recovery compared to monocytes. Overall, we found that LDGs are significantly less efficient at bacterial uptake compared to monocytes. Fig. 2A demonstrates a significant increase in the uptake of large bacterial quantities by monocytes compared to uptake by LDGs, as assayed using flow cytometry (Fig. 2A). A separate study describing LDGs as LDNs demonstrated that the

Journal of Cell Science (2021) 134, jcs252528. doi:10.1242/jcs.252528

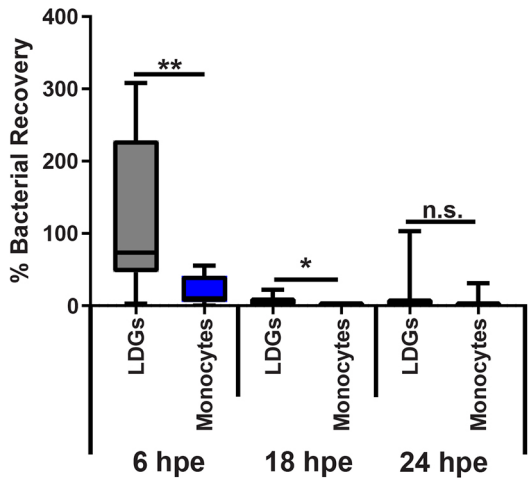

Fig. 1. LDGs are less efficient at bacterial elimination compared to monocytes. LDGs and monocytes isolated from human umbilical cord blood were infected with a MOI of ∼20 of *E. coli* O1:K1:H7 and incubated at 37°C for 1 h. The medium was replaced at this time point with fresh medium that contained gentamicin, and samples were incubated for an additional 2, 6, 18 and 24 h. At each time point, cells were permeabilized with 1% saponin, diluted tenfold, and plated for standard bacterial enumeration. The graph represents bacterial recovery for LDGs and monocytes at 6, 18 and 24 h post exposure (hpe). Data at all time points was normalized to that at 2 h for each cell type. The data shown are from five independent experiments, with median and interquartile range indicated. Statistical analysis was performed using a Mann–Whitney *U* test. **P*≤0.05; ***P*≤0.01; n.s. not significant.

LDNs, in contrast to NDNs, are unable to internalize *M. tuberculosis* (La Manna et al., 2019). Although our primary goal was to compare antibacterial activity of LDGs to that of a mononuclear cell abundantly recruited to sites of infection in an effort to determine their cumulative impact in bacterial clearance, we also compared internalization of bacteria between NDNs, LDGs and monocytes over time. We found that each cell type internalized a similar amount of bacteria at 30 min post infection (Fig. S3A). However, by 1.5–2 h, monocytes were the superior phagocyte (Fig. S3B). These results also demonstrate that LDGs and NDNs are comparable in their potential to phagocytose bacteria.

Since neonatal LDGs were limited in phagocytosis efficiency compared to monocytes, we further studied their ability to internalize bacteria at a range of bacterial densities. A multiplicity of infection (MOI) of 20 was required to achieve detection of fluorescent bacteria above background; increased rate of phagocytosis correlated with increasing MOI without saturation at an MOI of 200, further demonstrating inefficient phagocytosis (Fig. S4A,B). However, despite a poor rate of phagocytosis, the LDGs did traffic pHrodo-labeled bacteria to acidic compartments, similar to mononuclear phagocytes and other professional phagocytes, as observed by confocal microscopy (Fig. S4C, Movies 1 and 2). The number of fluorescent pHrodo particles phagocytosed per cell (Fig. 2B), as well as the area of pHrodo fluorescence per image (Fig. 2C) was significantly lower for LDGs compared to monocytes. To further study the kinetics of LDG and monocyte phagocytosis of bacteria and subsequent trafficking to acidified compartments, cells were infected and then longitudinally imaged over a 6 h period. The number of pHrodo^{+} bacteria per cell increased more gradually in LDGs than monocytes and peaked at 4 h (240 m, Fig. 2D). In contrast, internalization of bacteria by monocytes was more robust and continued to increase through 6 h of infection. Overall, these data suggest that although LDGs are able to internalize bacteria, they are unable to do so as efficiently as professional phagocytes during infection.

Low-density granulocytes express inflammatory cytokines during infection

Since LDGs have some ability to eliminate pathogens during infection, we wanted to determine whether this function is associated with a robust inflammatory response, compared to that of monocytes. Adult LDGs have been shown to upregulate immunosuppressive genes and inflammatory cytokines during cancer and bacterial infection (Janols et al., 2014; Holmgaard et al., 2015). However, the level of inflammatory cytokine production by neonatal LDGs and subsequent comparison to mononuclear phagocytes during infection has not been studied in depth. To determine whether LDGs express inflammatory cytokines at a level similar to monocytes during infection, we infected both cell types with *E. coli* and quantified IL-6, TNF-α, and IL-1-β expression at gene and protein levels. IL-6, IL-1-β and TNF-α cytokines are known biomarkers for sepsis in patients (Samraj et al., 2013; van der Poll et al., 2017). We found that infected LDGs were capable of producing inflammatory cytokines, but they did not mount a response as robust as that of infected monocytes (Fig. 3A). Secreted IL-6, TNF-α and IL-1-β cytokine levels were also significantly higher for infected monocytes compared to levels for infected LDGs (Fig. 3B–D). Overall, these data suggest that LDGs express inflammatory cytokine genes, but do not generate an inflammatory cytokine response comparable to monocytes during infection.

LDGs release DNA during infection

To our surprise, time-lapse imaging of LDGs cultured with bacteria identified thin extracellular structures that connected to other LDGs. Release of extracellular DNA traps is an important feature of neutrophil-mediated destruction of bacteria (Brinkmann et al., 2004; Papayannopoulos, 2018). We hypothesized that LDGs were releasing DNA into the extracellular space during infection. Using the nucleic acid stain Sytox Green, we identified abundant extracellular DNA strings released from what appeared to be dead or dying LDGs; their cellular integrity was compromised, as indicated by the availability of Sytox Green to the nuclear compartments (Fig. 4A; Movies 3 and 4). However, it is important to note that cellular viability was ∼90% for LDGs after 2 h in culture (Fig. S1C). The extracellular strings were eliminated in the presence of DNase I, indicating that they are composed of nucleic acids (Fig. 4A,B). In addition, these strings were scarcely observed in uninfected controls (Fig. 4B; Fig. S5A), suggesting that their production is increased during infection.

Citrullinated histones, in particular citrullinated histone H3 (CH3), are hallmarks of extracellular DNA production and have been used comprehensively to analyze neutrophil extracellular trap (NET) formation during infections (Wang et al., 2009; Lewis et al., 2015; Hirose et al., 2014). To investigate whether or not there was an increase in the presence of CH3, we prepared whole cell lysates from infected and control LDG cultures. Immunoblot analysis was performed to measure the abundance of CH3 proteins. We found that there was an increase in CH3 protein during bacterial infection as compared to levels in uninfected LDG cultures (Fig. 4C,D). This suggests that citrullinated histones are associated with the extracellular DNA produced by LDG during infection. PADI4 is a peptidyl arginine deiminase that is important for histone and DNA modification (Deplus et al., 2014; Chang and Fang, 2010) and has been used as a marker NET formation (Miller-Ocuin et al., 2019). To determine whether LDGs differentially express PADI4 during infection, we quantified *PADI4* gene expression at 1–1.5 h and 6 h post infection. We found similar levels of *PADI4* gene

Journal of Cell Science (2021) 134, jcs252528. doi:10.1242/jcs.252528

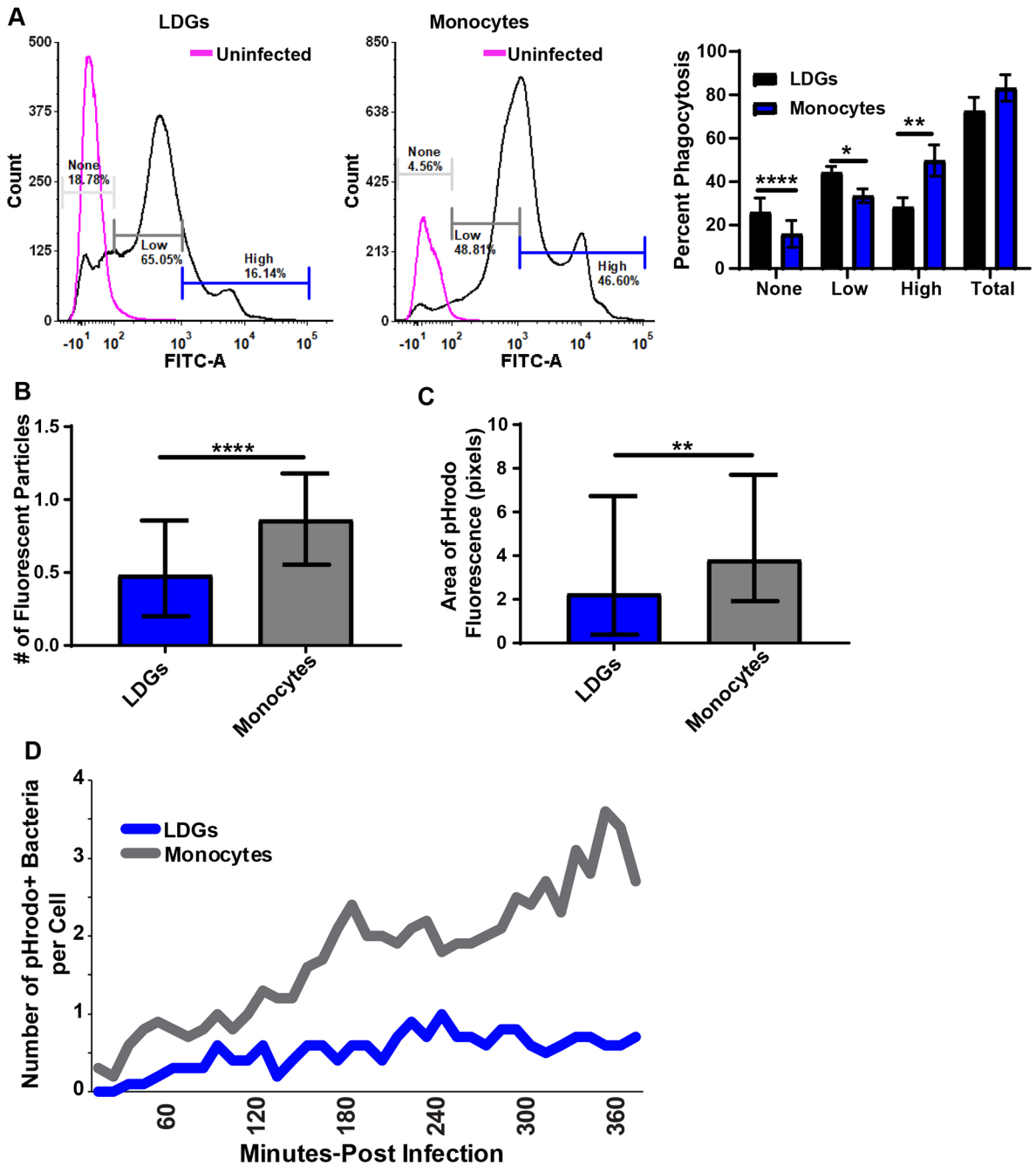

Fig. 2. LDGs are less efficient at bacterial uptake compared to monocytes. LDGs and monocytes isolated from human umbilical cord blood were infected with a MOI ~10 of Syto 9- or pHrodo Red-labeled *E. coli* O1:K1:H7 and incubated at 37°C. For flow cytometry, cells were fixed in 4% paraformaldehyde and resuspended in PBS prior to collection. For microscopy, cells were imaged at 1.5–2 h and analyzed for pHrodo fluorescence using FIJI. For longitudinal imaging, cells were imaged every 10 min over a 6 h period and pHrodo fluorescence quantified. (A) Representative flow cytometry histograms for LDGs (left) and monocytes (right), displaying the percentage of cells that have not phagocytosed bacteria (none), phagocytosed a low amount of bacteria (low) or phagocytosed a high amount of bacteria (high). Black, infected cells; magenta, uninfected cells. Bar chart (right) showing mean±s.e.m. percentage of each cell type in each phagocytosis category. Total indicates the sum of low phagocytosis and high phagocytosis for each cell type. Histograms and bar graphs are representative of a combined ten biological replicates. (B) Quantification of the number of pHrodo Red-labeled fluorescent bacterial particles phagocytosed by LDGs and monocytes during infection. *n*=63 and 70 images analyzed for LDGs and monocytes, respectively. Data from a combined three independent experiments are shown. (C) Quantification of the area in pixels of pHrodo Red fluorescence phagocytosed by LDGs and monocytes during infection. *n*=63 and 70 images analyzed for LDGs and monocytes, respectively. Data from a combined three independent experiments are shown. Data in B and C are as displayed as median and interquartile range. (D) Longitudinal phagocytosis of pHrodo-labeled bacteria during a 6 h timecourse is shown. Images were taken every 10 min of both LDGs (blue line) and monocytes (gray line). Number of fluorescent bacteria per cell for each cell type were quantified at each time point from nine fields of view. The graph shown is representative of two independent experiments. *n*=9 fields of view per cell type averaged at each time point. Statistical analysis was performed using a two-tailed, paired *t*-test (A) or a Mann–Whitney *U* test (B,C). **P*≤0.05, ***P*≤0.01, *****P*≤0.0001.

expression in both infected and uninfected LDGs at both time points (Fig. 4E; Fig. S5B). Additionally, we found similar *PADI4* gene expression in infected NDNs and LDGs at 1.5 h post infection (Fig. S5B). These results indicate that increased histone citrullination is independent of PADI4 transcription regulation in neonatal LDGs.

Journal of Cell Science (2021) 134, jcs252528. doi:10.1242/jcs.252528

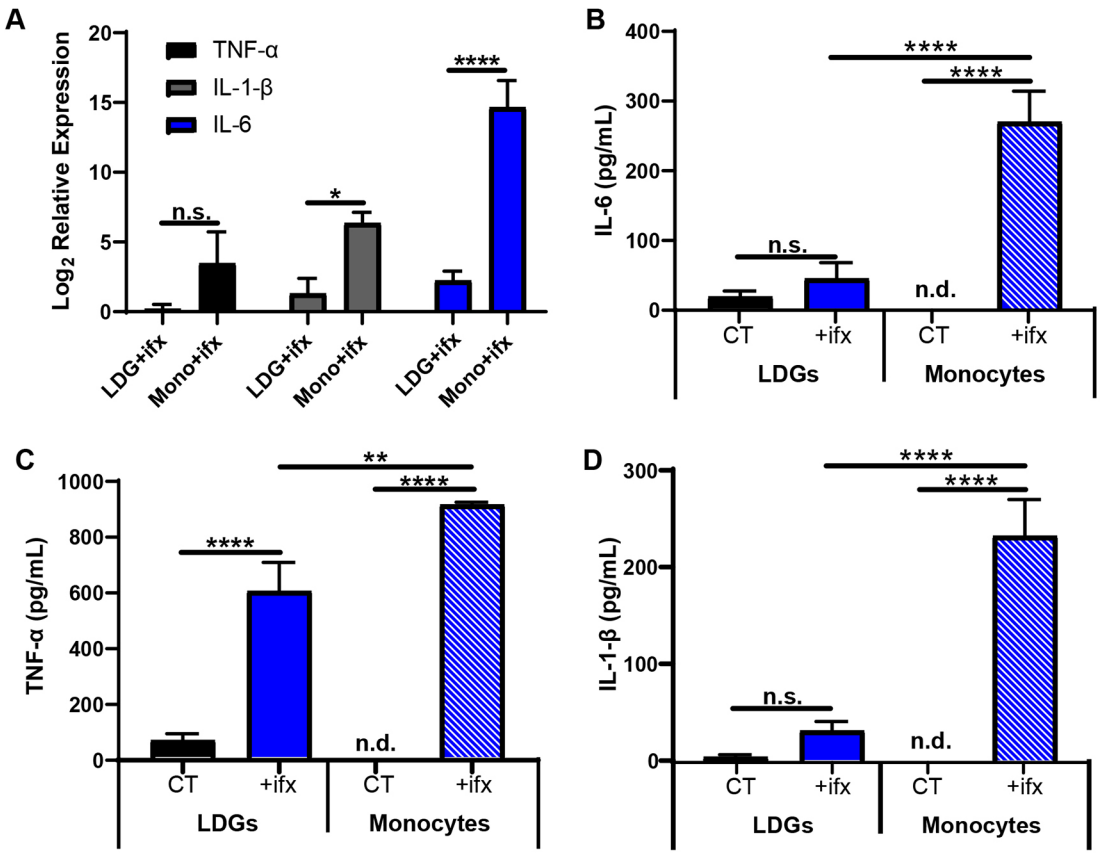

Fig. 3. LDGs express inflammatory cytokines at reduced levels compared to monocytes during infection. LDGs and monocytes isolated from human umbilical cord blood were infected with *E. coli* O1:K1:H7 at an MOI of ∼10 (ifx, infection) and incubated at 37°C for 6 h. Supernatants were collected for inflammatory cytokine measurements. Cells were then lysed in TRI Reagent for RNA extraction, cDNA synthesis and gene expression analysis of inflammatory cytokines. (A) Gene expression of IL-6, IL-1-β and TNF-α in LDGs and monocytes (mono) was normalized to GAPDH gene expression and expressed relative to uninfected controls. The data represent three combined experiments performed independently with 2–3 technical replicates each. Levels of (B) IL-6, (C) TNF-α and (D) IL-1-β proteins in culture supernatants were measured using ELISA for LDGs and monocyte infections in parallel (CT, control uninfected samples; n.d., not detected). The data shown represent four combined experiments performed independently with three technical replicates each. Data are presented as mean±s.e.m. Statistical analysis was performed using a one-way ANOVA with Sidak's multiple comparisons secondary test. *$P \leq 0.05$; **$P \leq 0.01$; ****$P \leq 0.0001$; n.s., not significant.

Extracellular DNA suppresses monocyte antibacterial activity

Brinkmann and colleagues (Brinkmann et al., 2004) were the first to demonstrate that adult NETs kill bacteria. To determine whether neonatal LDG extracellular DNA (eDNA) strings contribute to bacterial clearance, we performed a bacterial recovery assay to enumerate intracellular killing, along with standard plate counting of culture supernatants to account for extracellular bacterial killing in the presence or absence of DNase I. The extracellular and intracellular bacterial killing were analyzed individually as enumerated colony forming units (CFUs) (Fig. 5A,B). Although there was a trend toward increased bacterial numbers in the supernatant (Fig. 5A), and corresponding reduction in the recovery of bacteria from the intracellular compartment (Fig. 5B), the addition of DNase I did not significantly impact bacterial killing by LDGs (Fig. 5A,B). As expected, intracellular and extracellular bacterial killing was also unchanged by DNase I during monocyte infections (Fig. 5A,B). Overall, the bacterial killing experiments do not suggest that eDNA is potently anti-bacterial.

Since eDNA was not strongly associated with LDG-mediated killing of total bacteria, we explored whether or not eDNA had a regulatory effect on monocytes and impacted total bacterial clearance in the context of a mixed cell population. We co-cultured monocytes and LDGs together at a 1:1 ratio for 6 h with and without DNase I. At this time point, we quantified both extracellular and intracellular bacterial recovery by standard plate counting, as described above (Fig. 5A,B), and combined these numbers to enumerate the total bacterial burdens. When LDGs were co-cultured with monocytes, we found a significant decrease in total bacteria in the combined intracellular and extracellular compartments in the presence of DNase (Fig. 5C). This suggests an effect of the eDNA on monocyte killing of bacteria. Because the presence of eDNA was associated with a trend toward increased numbers of bacteria in the extracellular compartment, we hypothesized that eDNA may impair monocyte phagocytosis. To evaluate this possibility, we cultured LDGs with or without Syto 61-stained *E. coli* for 1 h and transferred the conditioned medium to monocytes subsequently infected with Syto 9-stained bacteria. The percentage phagocytosis of Syto 9-labeled bacteria was quantified by flow cytometry at 2 h. We found that monocyte phagocytosis of *E. coli* was significantly diminished when in the presence of LDG-infected conditioned medium that includes substantial eDNA (Fig. 5D). These data suggest that eDNA has an inhibitory effect on monocyte bacterial internalization. To determine the effect of LDG conditioned medium on monocyte activation and recruitment of other immune cells to sites of infection, we measured release of

Journal of Cell Science (2021) 134, jcs252528. doi:10.1242/jcs.252528

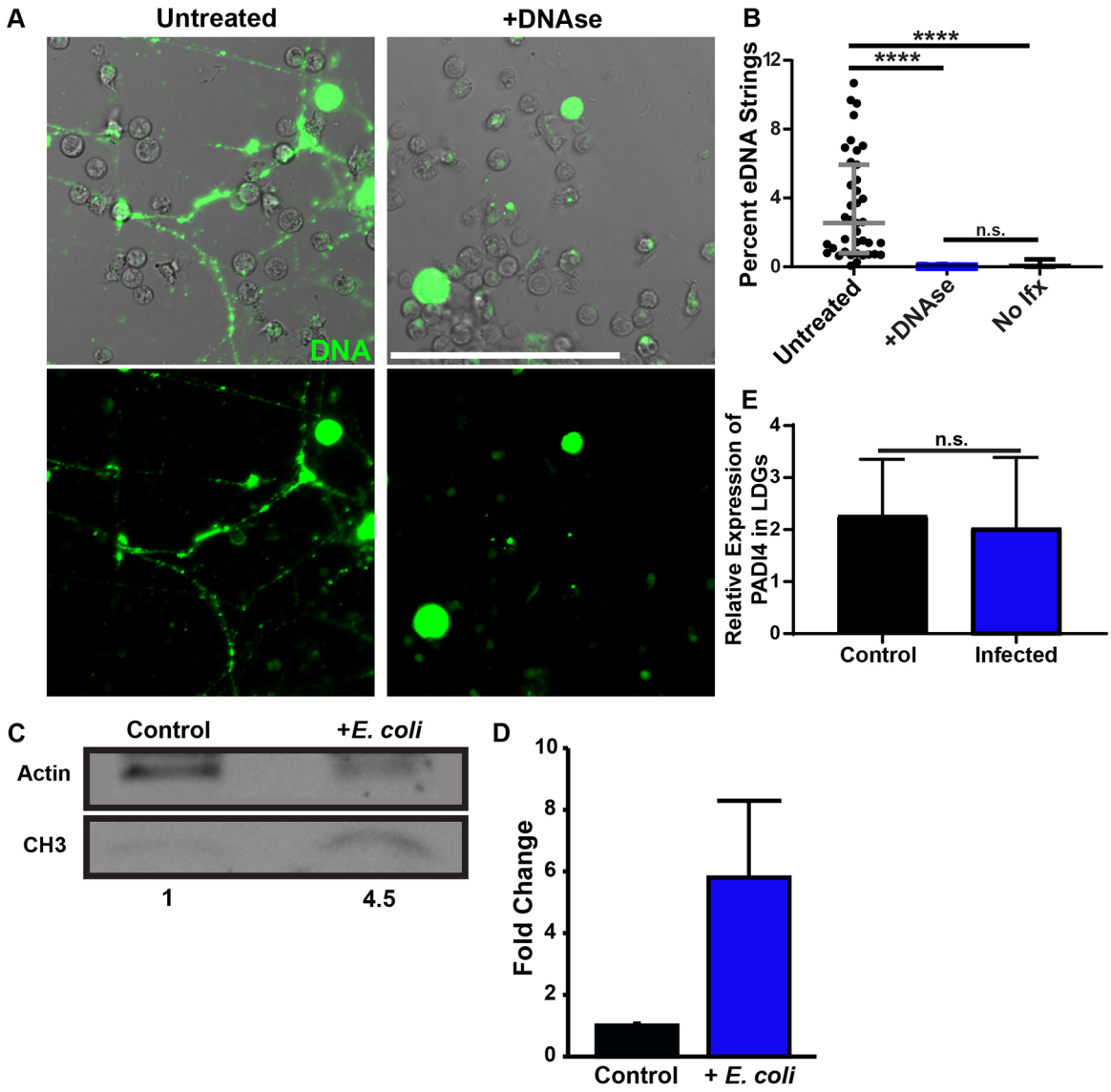

Fig. 4. LDGs release extracellular DNA during infection. LDGs isolated from human umbilical cord blood were infected with an MOI of ∼10 of *E. coli* O1:K1:H7 and incubated at 37°C for 1.5 h. To visualize extracellular DNA, Sytox Green (500 nM) was included. To degrade DNA, 100 U of DNase I was supplemented in the culture medium. (A,B) Cells were imaged on a Nikon A1R confocal microscope at 20×, and Sytox Green eDNA string fluorescence was quantified using Photoshop and FIJI. (A) Representative images and (B) quantification of the percentage area of each image containing Sytox Green eDNA string fluorescence from 2–3 combined experiments performed individually. *n*=39, 42 and 21 images for untreated, DNAse-treated, and uninfected (No Ifx) groups, respectively. Median with interquartile range is displayed. Statistical analysis was performed using a Kruskal–Wallis test with Dunn's multiple comparisons test. ****$P \leq 0.0001$; n.s., not significant. Scale bar: 100 µm. (C) A representative immunoblot of whole cell lysates showing CH3 and actin protein levels in control and infected (+*E. coli*) LDGs at 1.5 h. The numbers below the CH3 bands represent the fold change in CH3 protein for each sample. The blot is representative of three independent experiments. (D) Band density analysis for a combined three immunoblots performed separately; CH3 pixel intensities were normalized to actin controls for each experimental group. The fold increase in CH3 signal in infected LDGs is shown relative to the uninfected controls. Data are presented as mean±s.e.m. (E) Mean±s.e.m. ΔCt for PADI4 gene expression was normalized to that of GAPDH gene expression for uninfected and infected LDGs at 6 h. The data is representative of three combined experiments performed independently, with 2–3 technical replicates each. Statistical analysis was performed using a two-tailed, unpaired *t*-test (n.s., not significant).

IL-8 in infected monocytes cultured with or without conditioned medium. The IL-8 levels present in monocyte cultures were significantly lower in the presence of conditioned medium from infected LDGs (Fig. 5E). These data suggest that reduced bacterial killing by monocytes may be coupled with reduced cellular recruitment to sites of infection. The net effect may be to further compromise bacterial clearance. Overall, our data shows that LDGs can release extracellular DNA in association with citrullinated histone H3, although they do not potently contribute to direct bacterial killing, but rather contribute to inhibition of monocyte phagocytosis and bacterial killing. eDNA might lack antimicrobial components present in NET formation; however, it may have additional functions in host immunity during infection that remain to be fully understood.

DISCUSSION

Human gMDSCs have been well-studied in the context of cancer, but their direct involvement in host–pathogen interactions during infection has been less clear. There is even less understanding of LDN functionality or their distinction from gMDSCs in the context

Journal of Cell Science (2021) 134, jcs252528. doi:10.1242/jcs.252528

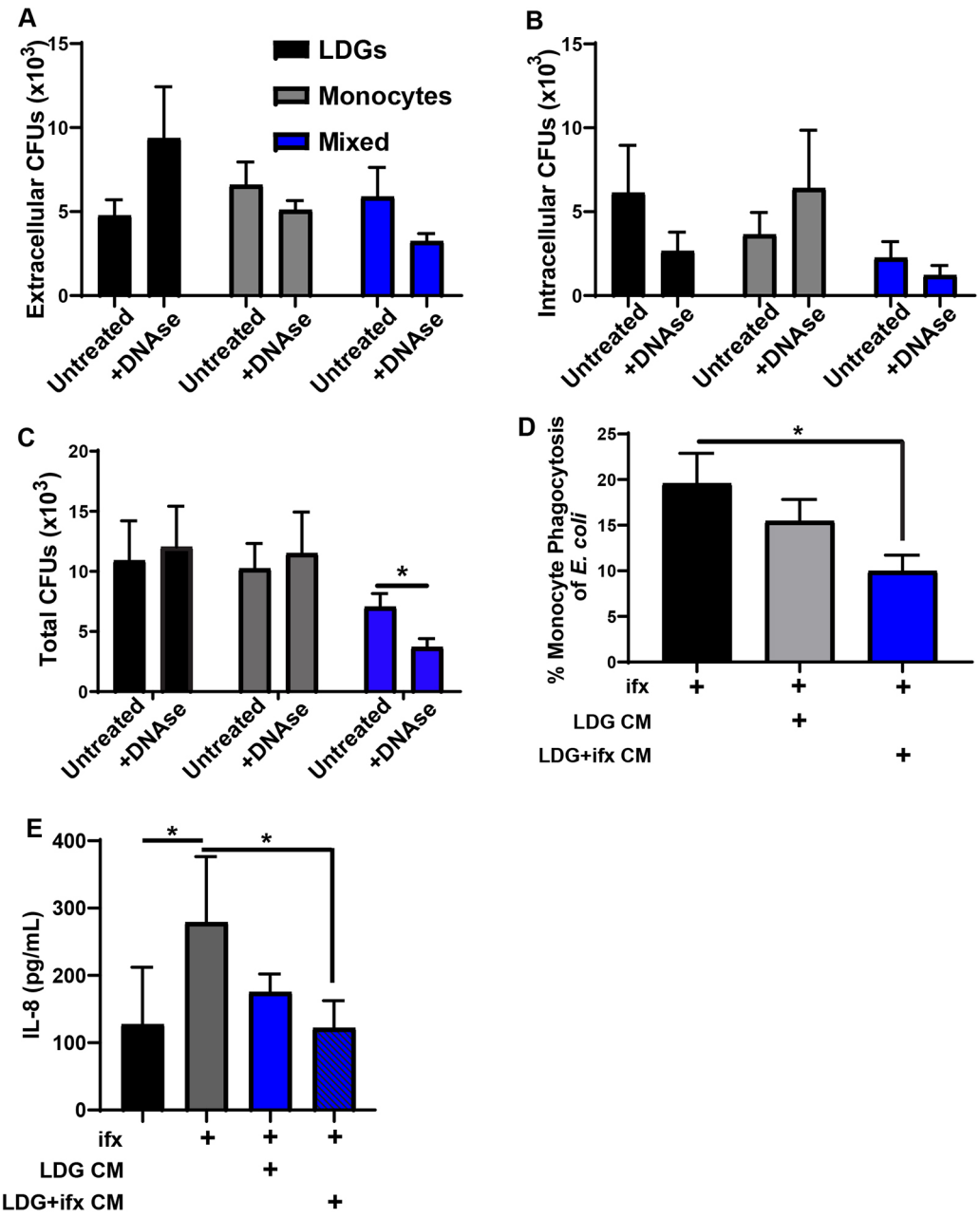

Fig. 5. The effect of LDG-derived eDNA on bacterial viability and on monocyte-mediated phagocytosis and killing of bacteria. LDGs and monocytes isolated from human umbilical cord blood were infected (ifx) with *E. coli* O1:K1:H7 at an MOI ∼10, either individually or during co-culture (mixed, LDGs+monocytes), and incubated at 37°C for 6 h. DNase I (100 U) was added to some cultures as indicated (+DNAse). (A–C) The mean±s.e.m. extracellular (A), intracellular (B) or combined (C) bacterial CFUs is shown for nine or ten biological replicates. (D) LDGs were infected with Syto 61-stained *E. coli* for 1 h. The conditioned culture medium was collected and transferred to monocytes. Monocytes were infected with Syto 9-stained *E. coli* immediately prior to the addition of LDG conditioned medium (CM). The mean±s.e.m. percentage phagocytosis of *E. coli* by monocytes in the presence or absence of infected (LDG+ifx CM) or uninfected LDG CM at 2 h is shown for three combined experiments performed separately with three technical replicates each. (E) LDGs were infected with *E. coli* for 1 h. The CM was collected and transferred to monocytes. Monocytes were infected with *E. coli* immediately prior to the addition of LDG CM and culture supernatants were analyzed at 6 h post infection for IL-8 protein levels using an ELISA. The mean±s.e.m. for three combined experiments performed separately with two technical replicates each is shown. Statistical analyses were performed using a two-way ANOVA (A,B), a Mann–Whitney test (C) or a one-way ANOVA with Dunnett's multiple comparisons (D,E). *$P \leq 0.05$.

of bacterial infection. Here, we describe the first in-depth studies on the direct interactions of LDG cells with bacteria, and the consequences to neighboring phagocytes in the local infectious milieu. Our findings rigorously demonstrate that human LDGs ($CD66^{hi}$, $CD33^{+}$, $CD14^{lo}$ and $HLA\text{-}DR^{-}$ cells that mildly suppress T cell proliferation) have the ability to phagocytose and kill bacteria, although at a reduced efficiency compared to monocytes. In addition to these functions, we observed release of DNA into the extracellular environment by LDGs during infection. This is in stark contrast to LDNs isolated from adult tuberculosis patients (La Manna et al., 2019), and suggests that LDGs from neonates have fundamentally different capability and activity levels. The eDNA is consistent with an increase in citrullination of histone H3, but does not significantly contribute to direct bacterial killing in

Journal of Cell Science (2021) 134, jcs252528. doi:10.1242/jcs.252528

LDG-only cultures. This result may highlight an important distinction from NDNs. However, our data shows that eDNA does have a significant impact on phagocytic function of monocytes during co-culture and following conditioned medium transfer and incubation. These activities are associated with a modest inflammatory response that does not rise to a level comparable with monocytes. A direct comparison of LDGs with mononuclear cells, as well as a characterization of their individual and combined abilities to kill bacteria during infection, has not previously been performed, and represents a void in the literature.

LDGs phagocytose *E. coli* O1:K1:H7 in a dose-dependent manner. Using both flow cytometry and confocal microscopy, we were able to rigorously establish that LDGs internalize bacteria and traffic them into acidic compartments, similar to professional phagocytes. We are the first to describe this pattern of intracellular trafficking in LDGs and to further study the consequences in a timecourse of bacterial killing. All other studies that have described bacteria within LDGs have done so without 3D reconstruction and cell surface/membrane staining to identify the exterior of the LDGs. This step is required to confirm intracellular localization. Furthermore, our study is the first to analyze the consequence of LDG phagocytosis of bacteria and corresponding inflammatory response, both fundamental aspects of LDG biology that have yet to be resolved completely (Leiber et al., 2017).

Leiber and colleagues have investigated the phagocytosis of a laboratory strain of *E. coli* by gMDSCs at a single MOI of 50 at one time point only (Leiber et al., 2017). Our study evaluated bacterial internalization at a range of MOIs in real time, describing the kinetics, and with a clinically relevant strain of *E. coli* responsible for invasive infections, such as sepsis and meningitis (Yao et al., 2006). Other studies have reported a lack of internalization of *M. tuberculosis*, or a reduced internalization of *S. aureus* bioparticles by LDNs (La Manna et al., 2019; Denny et al., 2010). Knaul et al. (2014) sorted $Ly6G^{+}Gr\text{-}1^{+}$ and $Ly6G^{-}Gr1^{int}$ cells from the lungs of mice infected with *M. tuberculosis* and imaged fluorescent bacteria within a subpopulation of these cells. These studies, while establishing an association with bacteria and internalization, did not address the requirements of bacterial density, intracellular localization, kinetics or efficiency of bacterial uptake. Our study rigorously addresses the frequency and abundance of internalization using flow cytometry and time-lapse confocal fluorescence microscopy, and compares this to that of professional phagocytes. La Manna et al. (2019) compared phagocytosis of *M. tuberculosis* amongst human LDNs and NDNs from adult patients finding no ability of LDNs to phagocytose *M. tuberculosis*. However, comparisons to a mononuclear cell in the same fraction of density gradient-centrifuged neonatal blood have not been performed. We further extended our approach to explore the fate of bacteria following internalization. He and colleagues reported enhanced killing of *E. coli* by monocytic and granulocytic MDSCs from mice, without procedural details that allow for interpretation (He et al., 2018). We expanded our comparisons to include neonatal NDNs, and found that LDGs and NDNs were comparable in their phagocytic function but less efficient relative to monocytes later during infection. Because our results do not demonstrate a defect in neonatal LDG phagocytosis function relative to that of NDNs, they are in contrast to the findings of La Manna et al. (2019). However, this may be explained by the different bacteria used and by differences between neonatal and adult cells. Overall, based on these prior studies, we are the first to establish that bacteria internalized by LDGs are trafficked to acidified compartments and to further measure bacterial killing over time.

Our results demonstrate that LDGs eliminate bacteria with reduced efficiency compared to monocytes, a comparison that had not previously been performed. Our analysis normalized the bacteria recovered to that internalized by each cell type at 2 h post gentamicin treatment to account for differences in uptake and to allow for direct comparison of the rate of killing. Cellular mechanisms responsible for reduced internalization and killing by LDGs compared to that by monocytes are currently unknown, although each function is independently impaired in LDGs. MDSCs and LDNs are both defined as immature myeloid cells (Hassani et al., 2020; Hsu et al., 2019), so there is potential for reduced expression of certain pattern recognition receptors (PRRs) or integrins on the surface that limits efficient internalization of bacteria. Additionally, CD14 is important in the recognition of lipopolysaccharide (LPS), a Gram-negative bacterial cell wall component (Pugin et al., 1994; Devitt et al., 1998). CD14 is highly expressed on monocytes and macrophages (Simmons et al., 1989; Ost et al., 2016), but the expression level is low on LDGs (Fig. S1B). There are no reports to date of complement receptor or mannose receptor expression levels on LDGs. These molecules, as well as the presence or absence of other markers normally found in higher abundance on granulocytes and monocytes, could be partly responsible for the reduced efficiency of phagocytosis by LDGs. To explain the reduced efficiency in bacterial clearance by LDGs, it is possible that although bacteria are trafficked to lysosomes, the kinetics of this response are delayed relative to those in professional phagocytes. This may also be influenced by reduced expression of molecules required for progression from early to late endosomes, or factors such as vacuolar ATPase that may limit the number of acidified compartments achievable within an LDG. Acidified compartments within MDSCs and LDGs may also have a more limited repertoire or abundance of hydrolytic molecules. Future studies will be necessary to further address the cell biology of LDGs and how it compares with that of professional phagocytes.

LDGs produce inflammatory cytokines during infection. Interestingly, each proinflammatory cytokine that we analyzed was produced at decreased levels in infected LDGs compared to levels in infected monocytes. TNF-α (*TNF*) gene expression at 6 h did not correlate with secreted cytokine levels at the same time point, suggesting that transcriptional activation peaks earlier during infection. This is in agreement with other studies suggesting that TNF-α is an 'immediate early gene' during infection (Falvo et al., 2010). TNF-α is also known to be regulated by posttranscriptional mechanisms such as AU-rich elements and microRNAs (Huang et al., 2012; Kontoyiannis et al., 1999; Espel, 2005). In a separate report, LDNs isolated from adult lupus patients have been shown to produce increased levels of TNF-α, type I interferons, and IFNγ compared to levels in NDNs from the same patients (Denny et al., 2010). This again highlights the potential that neonatal LDGs are fundamentally different from those of adults and/or cells isolated from individuals in different states (i.e. healthy versus infection versus lupus versus neonate) function uniquely. These types of differences have contributed to confusion and controversy surrounding LDGs, but rather may reflect that a 'one size fits all' definition or expectation of activity level is oversimplified. A range of neutrophil activity may exist similar to that described for macrophage polarization (Murray, 2017). Human gMDSCs have been shown to produce TGF-β, and both human and murine MDSCs express IL-10 (Leiber et al., 2017; Park et al., 2018; Bunt et al., 2009). We have also recently established that murine MDSCs are an important source of IL-27 during the neonatal period (Gleave Parson et al., 2019). Future studies will comprehensively analyze

Journal of Cell Science (2021) 134, jcs252528. doi:10.1242/jcs.252528

the expression of anti-inflammatory cytokines over a time range following exposure to a variety of bacteria to determine whether they are involved in limited inflammatory cytokine production by LDGs and are a sustained source of immune-suppressive factors during acute and chronic bacterial infections.

LDGs release extracellular DNA (eDNA) during infection. These results are novel, as other limited reports only describe release of eDNA during cancer or autoimmunity. Alfaro et al. (2016) have shown that gMDSCs produce eDNA in the tumor environment. However, it is worth noting that the cells described as gMDSCs in that study failed to exert any inhibition of T cell proliferation, traditionally considered a key characteristic of MDSCs. Other studies involving strictly adult LDNs have described eDNA formation in the context of autoimmune disease (Villanueva et al., 2011; Wright et al., 2017). LDGs from lupus patients exhibit increased NETosis compared to LDGs from control patients (Villanueva et al., 2011). Another study has suggested that adult LDNs do not form eDNA traps during infection with *M. tuberculosis* (La Manna et al., 2019). These discrepancies suggest that eDNA formations may be age-, disease- and/or microbe-dependent. At least some of the eDNA in our cultures appeared to be associated with cell death; Sytox Green should not have access to the nucleus in cells that maintain membrane integrity. Leiber et al. (2017) have reported an increased rate of apoptosis in neonatal MDSCs infected with *E. coli*. Our observations are not consistent with an apoptotic form of cell death. The nature of this difference in findings is not clear, but may be influenced by the virulence of the bacteria. The eDNA was associated with a slight reduction in bacterial viability during LDG culture alone, but the overall magnitude was not striking. Granule-packed adult neutrophils generate NETs that are strongly antibacterial (Brinkmann et al., 2004; Li et al., 2010). One possible explanation for limited bactericidal activity may be due to a lower granule content in LDGs compared to neutrophils (Rosales, 2018). Neutrophil granules are packed with highly antimicrobial contents, including defensins, cathepsins and proteinases, and are released alongside eDNA during NET formation (Borregaard et al., 2007). To our knowledge, there are few studies that describe the contents of the granules found in gMDSCs or LDNs. Of those, some suggest that there are much lower expression levels of granule proteins in gMDSCs compared to bone-marrow-derived cells, as well as lower expression of NADPH subunits and peroxidases (Pillay et al., 2013). However, it is known that MDSCs do express some proteins that are found in the granules of NDNs, including arginase I and myeloperoxidase (MPO), although the subcellular location remains unknown (Youn et al., 2012; Rodriguez et al., 2009). Similarly, evidence of granular proteins, including elastase and MPO, was obtained from lupus patient LDNs, and these cells may have disease-specific characteristics (Villanueva et al., 2011; Wirestam et al., 2019). Future experiments that explore the contents of LDG granules and their association with eDNA compared to NDNs will help improve our understanding of the role and toxicity of eDNA. Additional studies that incorporate high-resolution microscopy will be necessary to visualize bacteria in association with eDNA and other associated components.

In addition to the limited bactericidal activity of eDNA, we found that the presence of eDNA in co-cultures with monocytes significantly reduced bacterial killing. Monocyte bacterial uptake was also significantly inhibited in the presence of infected LDG-conditioned medium, further supporting an influence on antibacterial activity. These results are exciting and suggest that LDG-derived eDNA may inhibit physical interaction of the monocytes with bacteria, slowing internalization and killing. These data are in agreement with Dietz et al. (2019), who found that monocytes cultured in the presence of MDSCs exhibit reduced expression of phagocytosis receptors with a modest impact on bacterial internalization. Our *in vitro* findings raise the question of whether this influence may be more profound in the *in vivo* setting and potentially impair bacterial clearance during infection. Neutrophil eDNA has been implicated in endothelial cell damage and death (Gupta et al., 2010; Clark et al., 2007). Additionally, extracellular histones, such as citrullinated histone H3, cause damage to multiple cell types and contribute to organ failure (Kutcher et al., 2012). Histone release during sepsis can also promote endothelial cell dysfunction, hypoxia in tissues and cell death (Wildhagen et al., 2014; Xu et al., 2009). It is possible that eDNA may also harbor similar cytotoxic activities towards host cells, even if at a lesser degree. However, we also acknowledge that eDNA may not have all the components present in NETs. We demonstrated the presence of citrullinated histones in LDG cell lysates, but *PADI4* gene expression was unchanged during infection. This may suggest that CH3 is less abundant relative to levels in NDN traps, and that would be consistent with reduced antibacterial activity of eDNA. However, it is also possible that histone citrullination in LDGs is not fully regulated by changes in PADI4. It is worth noting that human NDNs have also been shown to undergo NETosis without activation of PADI4 and detectable histone deiminase (Neeli and Radic, 2013). Additional studies will need to be conducted to fully characterize the content of eDNA, cellular pathways that influence regulation and association with cell death processes, and its effect on innate and adaptive immune function.

Our *in vitro* experiments have limitations, and it is important to note that our experiments do not, and cannot, model all aspects of the *in vivo* scenario. We set out to understand how LDGs may contribute to the microenvironment of infection through their direct interactions with bacteria, as well as their interactions with other professional phagocytes that would be found or recruited to a site of infection. With an *in vitro* model, we are not able to account for all cell types that would be present in the local infectious milieu. Given the limitations in distinguishing LDGs from NDNs or highly suppressive MDSCs based on surface markers, it would be a significant challenge to reliably identify these different cell types at the tissue level and to further understand their functionality in the way that we have studied them mechanistically in this report. Our experiments explored the effect of conditioned medium from control or infected LDGs on the ability of monocytes to release the chemotactic cytokine IL-8, and they suggest that monocytes co-cultured with LDGs releasing eDNA are not further activated to increase recruitment of other innate or adaptive immune cells. However, we acknowledge that this experimental design does not fully encapsulate an *in vivo* environment with abundant inflammatory and anti-inflammatory signals or multiple immune cell types present during infection. Additionally, in the context of comparisons amongst immune cell types, both LDGs and NDNs are unable to thrive post freeze-thaw. Any studies incorporating these cell types must use fresh blood for isolation, and this limits the types of comparisons that can be made (e.g. macrophages differentiated from blood monocytes can take 5–7 days to fully differentiate). Although these and other unstated limitations occur during *in vitro* studies, they do not undermine the importance of *in vitro* studies overall. Our work is dedicated to characterizing the important

Journal of Cell Science (2021) 134, jcs252528. doi:10.1242/jcs.252528

aspects of LDGs in the context of direct pathogen contact and their effects on other immune cells during infection. This work has allowed us to further understand how LDGs interact with other immune components and immune cells during host–pathogen interactions that were previously unknown. Additionally, we have also shown that LDGs do have some functional differences from NDNs that were previously unreported. These insights would have been challenging to study in an *in vivo* situation.

Throughout this study and the subsequent literature review, we have discovered an important, but unresolved, issue in the lack of immunophenotypic characterization of LDGs. We are not the first to raise this issue; others have described concerns about the inability to definitively separate human LDNs from gMDSCs in Ficoll density gradients (Jablonska and Granot, 2017; Ui Mhaonaigh et al., 2019). To date, there is no definitive marker that can differentiate LDNs from gMDSCs, and thus studies in which LDNs or gMDSCs are 'definitively' defined may in fact be a mixture of both populations. Multiple studies have also suggested that LDNs and gMDSCs exhibit very similar expression and abundance of cell surface markers, including being HLA-DR^{-}, CD14$^{lo/-}$, CD33^{+} and CD66^{+} (Cassetta et al., 2019; Moses and Brandau, 2016). These markers are used in our study, and for clarity, we define our population as LDGs, embracing the uncertainty within the field. However, our study brings to light the importance of this cellular population in regulating innate immunity to bacterial infection, and lobbies for consideration of the source of cells, accounting for species, age, infection and other disease states. Specifically for neonatal blood, the method of birth (i.e. cesarean or vaginal) and the potential impact of analgesics and narcotics during labor on leukocytes in the mother and baby may also account for discrepancies noted in different studies of LDGs (Rizzo et al., 2011). We also suggest that inhibition of T cell proliferation is not the only measure of immune suppression. Our data demonstrate a mild suppression of T cell proliferation in the presence of neonatal LDGs. This is in contrast to other studies that claim a heightened suppression of T cell proliferation by MDSCs (Rieber et al., 2013b; Leiber et al., 2017). Does that mean our cells are LDNs? Discrepancies between studies on LDNs have also been noted. For instance, La Manna et al. (2019) suggest that adult LDNs cannot phagocytose bacteria (*M. tuberculosis*), and do not produce extracellular traps in the presence of *M. tuberculosis*; however, another study has found that adult LDNs are able to phagocytose bacteria (*S. aureus* particles) and have an increased ability to produce extracellular DNA traps (Denny et al., 2010). This data, in addition to our data on the phagocytosis of *E. coli* O1:K1:H7, suggests that these LDN populations may be microbe-dependent in the context of phagocytic function. Future studies will need to address novel ways to separate LDNs from gMDSCs in density gradients, if possible, and to further establish functional standards for cell description.

In conclusion, we have demonstrated that neonatal LDGs possess the ability to phagocytose, traffic to lysosomes and kill bacteria during acute infection. This is not associated with a robust inflammatory response relative to monocytes. Additionally, we have unexpectedly discovered that LDGs release eDNA that is not directly antibacterial, but that has an impact on monocyte-mediated bacterial internalization and clearance during co-culture infections and within infections exposed to LDG infected medium. Ongoing work in our lab aims to further characterize eDNA and its involvement in LDG interactions with bacteria and other immune cells during infection. Enhanced understanding of LDG activities may direct the development of novel therapies to improve neonatal immunity and disease outcome during severe infections.

MATERIALS AND METHODS

Cell culture

Human umbilical cord blood was obtained from the Cleveland Cord Blood Center and Ruby Memorial Hospital (Morgantown, WV) under West Virginia University Institutional Review Board (IRB) approval. Blood was donated from healthy infants of gestational age ≥37 weeks. All donors are anonymous and de-identified. Whole blood was centrifuged at 1500 ***g*** for 10 min to obtain buffy coats. Buffy coats were further subjected to Ficoll (GE Healthcare Life Sciences, Chicago, IL) density gradient centrifugation at 400 ***g*** for 30 min to isolate cord blood mononuclear cells (CBMCs). CD66abce^{+} LDGs, CD4^{+} T cells and CD8^{+} T cells were isolated by immunomagnetic selection using their respective Miltenyi Biotec isolation reagents (Miltenyi Biotec, Bergisch Gladbach, Germany). Monocytes were isolated through Optiprep (StemCell Technologies, Vancouver, British Columbia, Canada) density gradient centrifugation of CBMCs at 600 ***g*** for 25 min, as described previously (Kraft et al., 2013). NDNs were isolated from blood pellets post-Ficoll centrifugation using 0.225% saline lysis (Ricca, Arlington, TX). CD66abce^{+} NDNs were isolated by immunomagnetic selection using Miltenyi Biotec isolation reagents (Miltenyi Biotec, Bergisch Gladbach, Germany). LDGs, NDNs and monocytes were incubated at a concentration of 1×10^{5}–9×10^{5} cells/well in FluoroBrite Dulbecco's Modified Eagle Medium (DMEM, Thermo Fisher Scientific, Waltham, MA) supplemented with 10% human serum (Gemini Bioproducts, West Sacramento, CA), 25 mM HEPES and 2 mM L-glutamine. T cells were cultured at a concentration of 1×10^{5}–3×10^{5} cells/well in RPMI-1640 (Mediatech, Manassas, VA), supplemented with 10% human serum, 100 U ml^{-1} penicillin/streptomycin, 2 mM L-glutamine, 25 mM HEPES, 1 mM sodium pyruvate and 0.05 mM 2-mercaptoethanol. Human cell cultures were incubated at 37°C in 24-, 48- or 96-well tissue culture-treated plastic-bottom plates, or in a 35 mm ibidi Quad µ-Dish (ibidi, Fitchburg, WI) for confocal and/or epifluorescence imaging.

Fluorescent labeling and bacterial infection

Human LDGs, NDNs and/or monocytes were infected at a MOI of ∼2–200 of *Escherichia coli* strain O1:K1:H7. The bacteria were taken from pre-titered frozen cultures and washed in phosphate-buffered saline (PBS; Corning, Manassas, VA), centrifuged at 2000 ***g*** for 5 min, and resuspended in a volume equivalent to an inoculum of 50 µl/well. Bacteria were labeled with 5–20 µM Syto 9 Green Fluorescent Nucleic Acid Stain, 5–20 µM Syto 61 Red Fluorescent Nucleic Acid Stain or 500 µM pHrodo Red SE (Thermo Fisher Scientific, Waltham, MA) and washed 3–5 times with PBS prior to infection. For extracellular bacterial recovery assays, bacteria were taken directly from culture supernatants, diluted tenfold in PBS, and enumerated by standard plate counting on tryptic soy agar (TSA; Becton, Dickinson and Company, Sparks, MD) incubated at 37°C overnight. To visualize extracellular DNA, 500 nM of Sytox Green Nucleic Acid Stain (Thermo Fisher Scientific, Waltham, MA) was added prior to microscopy. In experiments incorporating DNase I, the medium was supplemented with 100 units of DNase I (Roche, Basel, Switzerland).

Gentamicin protection assay

Human LDGs and monocytes were infected at an MOI of ∼20 for 1 h at 37°C. At 1 h post infection, supernatants were discarded and cells were supplemented with new medium containing 100 µg ml^{-1} gentamicin (Quality Biological, Gaithersburg, MD) to eliminate extracellular bacteria. Cells were incubated for 2, 6, 18 and 24 h, and then permeabilized using 1% saponin in PBS (MP Biomedicals, Solon, OH). Cell lysates were diluted tenfold in PBS, and bacteria were enumerated by standard plate counting.

Flow cytometry

Cells and bacteria were incubated at 37°C for varying time points. At each time point, cells were collected in 500 µl of 4% paraformaldehyde (Affymetrix, Cleveland, OH) and kept at 4°C until use. Cells were resuspended in 400 µl PBS and ∼10,000 events were collected on an LSRFortessa (Becton, Dickinson and Company, Sparks, MD). Percentage of cells gated in FITC- (488 nm laser, 490/525 nm excitation/emission), PE- (561 nm laser, 496/578 nm excitation/emission) or Pacific Blue/Alexa Fluor

405- (405 nm laser, 410/455 nm excitation/emission) channels were used for data analysis. For cell marker profiling, LDGs were immunolabeled with PE-conjugated anti-HLA-DR (cat. # 12-9956-42, clone LN3; Invitrogen, San Diego, CA), anti-human CD66b-PE (cat. # 305105, clone G10F5; BioLegend, San Diego, CA), FITC-conjugated anti-CD14 (cat. # FAB3832P, clone 134620; R&D Systems, Minneapolis, MN) and FITC-conjugated anti-CD33 (cat. # 303303, clone HIM3-4; BioLegend, San Diego, CA). All antibodies were diluted according to manufacturer specifications.

Immunoblot analysis

LDGs at a concentration of 4×10^5–5×10^5 cells/well were infected with an MOI of ∼10 of *E. coli* in a 96-well plate and incubated at 37°C. Cell lysates were prepared at 1.5 h post infection using RIPA buffer supplemented with protease inhibitor cocktail and phenylmethylsulfonyl fluoride (PMSF) (Santa Cruz Biotechnology, Dallas, TX). Equal amounts of cell lysates were separated on SDS–PAGE gels (Bio-Rad, Hercules, CA) and transferred to a nitrocellulose membrane (GE Healthcare Life Sciences, Chicago, IL) by standard techniques. Primary antibodies used in this study were rabbit polyclonal anti-histone H3 (citrulline R2+R8+R17) antibody (cat. # ab5103, lot # GR3263131-3; Abcam, Cambridge, MA) and rabbit polyclonal anti-actin N-terminal antibody (cat. # A2103, lot # 051M4767; Sigma Aldrich, St Louis, MO). Primary antibody binding was revealed using horseradish peroxidase-conjugated polyclonal goat anti-rabbit IgG secondary antibody (cat. # sc-2004, lot # B0513; Santa Cruz Biotechnology, Dallas, TX; cat. # 4055-05, lot # D1812-Y099; SouthernBiotech, Birmingham, AL). All antibodies were diluted according to manufacturer specifications. SuperSignal West Femto Maximum Sensitivity Substrate (Thermo Fisher Scientific, Waltham, MA) was applied to visualize proteins imaged on a ChemiDoc Touch Gel Imaging System (Bio-Rad, Hercules, CA). To quantify the band density for each sample, each band was clipped at the same dimensions in Adobe Photoshop. Images were then opened in ImageJ (FIJI, https://fiji.sc/), kept at the same pixel threshold, made binary and measured for pixels and percent area.

T cell proliferation assay

$CD4^+$ or $CD8^+$ T cells were stained with 5 µM CellTrace Violet (Thermo Fisher Scientific, Waltham, MA) for 20 min at 37°C. The labeling was quenched with 10% fetal bovine serum (FBS; Gemini Bio-Products, West Sacramento, CA) in PBS and cells were resuspended in T cell medium. Cells were then plated at 1×10^5–3×10^5 cells/well in a non-tissue culture treated 96-well plate (Corning, Corning, NY) and incubated for 2 h at 37°C. $CD66^+$ LDGs were then added at a 1:1 concentration to T cells. To promote T cell proliferation, the cultures were supplemented with 100 units of IL-2 (Shenandoah Biotech, Warwick, PA) or 1×10^5–3×10^5 CD3/CD28 Dynabeads/well (Thermo Fisher Scientific, Waltham, MA). The cultures were incubated at 37°C and cells were harvested each day through 4 days and fixed in 4% paraformaldehyde until analyzed by flow cytometry.

Quantitative real-time PCR

LDGs, NDNs and monocytes were cultured with or without *E. coli* at a MOI of ∼10 in 48- or 24-well plastic-bottom plates for 1–1.5 or 6 h. At each time point, cells were resuspended in 200–300 µl of TRI Reagent (Molecular Research Center, Cincinnati, OH; Sigma, St Louis, MO) and RNA was isolated according to the manufacturer's protocol. First-strand cDNA was synthesized using the iScript cDNA synthesis kit (Bio-Rad, Hercules, CA). Quantitative PCR reactions included cDNA diluted twofold, gene-specific Taqman primer probe sets (Applied Biosystems, Foster City, CA) and iQ Supermix (Bio-Rad, Hercules, CA). Cycling was performed in triplicate using a Step One Plus Real Time detection system (Applied Biosystems, Foster City, CA). Gene-specific amplification was normalized to GAPDH as an internal reference gene and expressed as $\log_2$ relative gene expression using the formula $2^{-\Delta\Delta Ct}$.

Cytokine measurements

Supernatants from infections were collected and clarified by standard techniques. IL-6, IL-1-β, IL-8 and TNF-α protein levels were measured in duplicate using Ready-Set-Go! ELISA kits (eBioscience, San Diego, CA) or Invitrogen ELISA kits (Thermo Fisher Scientific, Waltham, MA). Protein concentrations were determined relative to standards assayed in parallel.

Fluorescence microscopy

A Nikon A1R confocal microscope was used for confocal and epifluorescence imaging (Nikon, Melville, NY). Objective lenses with powers of 20× [numerical aperture (NA), 0.75], 40× (oil, NA, 1.3), and 60× (oil, NA, 1.4) were used. Images are overlays of differential interference contrast (DIC) and fluorescence images or fluorescence image panels. Syto 9/Sytox Green and pHrodo Red were detected by optical lasers and filters for excitation/emission at 490/525 nm (FITC) and 555/580 nm (TRITC), respectively. Images in Fig. 2 were analyzed in FIJI. Briefly, images were thresholded for bacterial fluorescence, and each area was quantified with identical settings per experiment and processed identically. For analysis of eDNA strings, images were processed using Photoshop (CC, version 20.0.8, 64 bit; Adobe Systems Incorporated) and FIJI. Briefly, each image was opened in Photoshop and eDNA strings were manually outlined using a black pen tool (size 9, 100% opacity). The manually labeled layers were then transferred to FIJI, made binary and the area of string outline (the black lines) was quantified for each image. For 6-h time lapses, cells were imaged on a Lionheart FX automated microscope (BioTek, Winooski, VT). Images were acquired using a 20× objective (NA, 0.45) and analyzed using Gen5 Image+ software (version 3.05.11; BioTek, Winooski, VT).

Statistical analysis

All statistical analyses were performed using GraphPad Prism software (version 8; La Jolla, CA). Data was tested using non-parametric or parametric measures, as indicated in the figure legends.

Acknowledgements

We would like to thank members of the Robinson lab for stimulating discussions, Dr Matthew Daddysman for help with Gen5 Image+ image analysis, Drs Amanda Ammer and Karen Martin for microscopy guidance, and Dr Kathy Brundage for flow cytometry guidance.

Competing interests

The authors declare no competing or financial interests.

Author contributions

Conceptualization: B.G.S., C.M.R.; Methodology: B.G.S., S.M.A., C.M.R.; Validation: C.M.R.; Formal analysis: B.G.S., J.K.V., C.M.R.; Investigation: B.G.S., C.M.R.; Resources: S.M.A., C.M.R.; Data curation: B.G.S.; Writing - original draft: B.G.S.; Writing - review & editing: B.G.S., S.M.A., C.M.R.; Visualization: B.G.S.; Supervision: C.M.R.; Project administration: C.M.R.; Funding acquisition: C.M.R.

Funding

This work was supported by West Virginia University institutional funds.

Supplementary information

Supplementary information available online at
https://jcs.biologists.org/lookup/doi/10.1242/jcs.252528.supplemental

References

Alfaro, C., Teijeira, A., Oñate, C., Pérez, G., Sanmamed, M. F., Andueza, M. P., Alignani, D., Labiano, S., Azpilikueta, A., Rodriguez-Paulete, A. et al. (2016). Tumor-produced Interleukin-8 attracts human myeloid-derived suppressor cells and elicits extrusion of Neutrophil Extracellular Traps (NETs). *Clin. Cancer Res.* **22**, 3924-3936. doi:10.1158/1078-0432.CCR-15-2463

Borregaard, N., Sørensen, O. E. and Theilgaard-Mönch, K. (2007). Neutrophil granules: a library of innate immunity proteins. *Trends Immunol.* **28**, 340-345. doi:10.1016/j.it.2007.06.002

Bowers, N. L., Helton, E. S., Huijbregts, R. P. H., Goepfert, P. A., Heath, S. L. and Hel, Z. (2014). Immune suppression by neutrophils in HIV-1 infection: role of PD-L1/PD-1 pathway. *PLoS Pathog.* **10**, e1003993. doi:10.1371/journal.ppat.1003993

Brinkmann, V., Reichard, U., Goosmann, C., Fauler, B., Uhlemann, Y., Weiss, D. S., Weinrauch, Y. and Zychlinsky, A. (2004). Neutrophil extracellular traps kill bacteria. *Science* **303**, 1532-1535. doi:10.1126/science.1092385

Bronte, V., Apolloni, E., Cabrelle, A., Ronca, R., Serafini, P., Zamboni, P., Restifo, N. P. and Zanovello, P. (2000). Identification of a CD11b(+)/Gr-1(+)/

CD31(+) myeloid progenitor capable of activating or suppressing CD8(+) T cells. *Blood* **96**, 3838-3846. doi:10.1182/blood.V96.12.3838

Bronte, V., Brandau, S., Chen, S.-H., Colombo, M. P., Frey, A. B., Greten, T. F., Mandruzzato, S., Murray, P. J., Ochoa, A., Ostrand-Rosenberg, S. et al. (2016). Recommendations for myeloid-derived suppressor cell nomenclature and characterization standards. *Nat. Commun.* **7**, 12150. doi:10.1038/ncomms12150

Brudecki, L., Ferguson, D. A., McCall, C. E. and El Gazzar, M. (2012). Myeloid-derived suppressor cells evolve during sepsis and can enhance or attenuate the systemic inflammatory response. *Infect. Immun.* **80**, 2026-2034. doi:10.1128/IAI.00239-12

Bunt, S. K., Clements, V. K., Hanson, E. M., Sinha, P. and Ostrand-Rosenberg, S. (2009). Inflammation enhances myeloid-derived suppressor cell cross-talk by signaling through Toll-like receptor 4. *J. Leukoc. Biol.* **85**, 996-1004. doi:10.1189/jlb.0708446

Carmona-Rivera, C. and Kaplan, M. J. (2013). Low-density granulocytes: a distinct class of neutrophils in systemic autoimmunity. *Semin. Immunopathol.* **35**, 455-463. doi:10.1007/s00281-013-0375-7

Cassetta, L., Baekkevold, E. S., Brandau, S., Bujko, A., Cassatella, M. A., Dorhoi, A., Krieg, C., Lin, A., Loré, K., Marini, O. et al. (2019). Deciphering myeloid-derived suppressor cells: isolation and markers in humans, mice and non-human primates. *Cancer Immunol. Immunother.* **68**, 687-697. doi:10.1007/s00262-019-02302-2

Chang, X. and Fang, K. (2010). PADI4 and tumourigenesis. *Cancer Cell Int.* **10**, 7. doi:10.1186/1475-2867-10-7

Chen, J., Ye, Y., Liu, P., Yu, W., Wei, F., Li, H. and Yu, J. (2017). Suppression of T cells by myeloid-derived suppressor cells in cancer. *Hum. Immunol.* **78**, 113-119. doi:10.1016/j.humimm.2016.12.001

Clark, S. R., Ma, A. C., Tavener, S. A., McDonald, B., Goodarzi, Z., Kelly, M. M., Patel, K. D., Chakrabarti, S., McAvoy, E., Sinclair, G. D. et al. (2007). Platelet TLR4 activates neutrophil extracellular traps to ensnare bacteria in septic blood. *Nat. Med.* **13**, 463-469. doi:10.1038/nm1565

Davis, R. J., Silvin, C. and Allen, C. T. (2017). Avoiding phagocytosis-related artifact in myeloid derived suppressor cell T-lymphocyte suppression assays. *J. Immunol. Methods* **440**, 12-18. doi:10.1016/j.jim.2016.11.006

Denny, M. F., Yalavarthi, S., Zhao, W., Thacker, S. G., Anderson, M., Sandy, A. R., McCune, W. J. and Kaplan, M. J. (2010). A distinct subset of proinflammatory neutrophils isolated from patients with systemic lupus erythematosus induces vascular damage and synthesizes type I IFNs. *J. Immunol.* **184**, 3284-3297. doi:10.4049/jimmunol.0902199

Deplus, R., Denis, H., Putmans, P., Calonne, E., Fourrez, M., Yamamoto, K., Suzuki, A. and Fuks, F. (2014). Citrullination of DNMT3A by PADI4 regulates its stability and controls DNA methylation. *Nucleic Acids Res.* **42**, 8285-8296. doi:10.1093/nar/gku522

Devitt, A., Moffatt, O. D., Raykundalia, C., Capra, J. D., Simmons, D. L. and Gregory, C. D. (1998). Human CD14 mediates recognition and phagocytosis of apoptotic cells. *Nature* **392**, 505-509. doi:10.1038/33169

Dietz, S., Schwarz, J., Vogelmann, M., Spring, B., Molnár, K., Orlikowsky, T. W., Wiese, F., Holzer, U., Poets, C. F., Gille, C. et al. (2019). Cord blood granulocytic myeloid-derived suppressor cells impair monocyte T cell stimulatory capacity and response to bacterial stimulation. *Pediatr. Res.* **86**, 608-615. doi:10.1038/s41390-019-0504-7

Dumitru, C. A., Moses, K., Trellakis, S., Lang, S. and Brandau, S. (2012). Neutrophils and granulocytic myeloid-derived suppressor cells: immunophenotyping, cell biology and clinical relevance in human oncology. *Cancer Immunol. Immunother.* **61**, 1155-1167. doi:10.1007/s00262-012-1294-5

Espel, E. (2005). The role of the AU-rich elements of mRNAs in controlling translation. *Semin. Cell Dev. Biol.* **16**, 59-67. doi:10.1016/j.semcdb.2004.11.008

Falvo, J. V., Tsytsykova, A. V. and Goldfeld, A. E. (2010). Transcriptional control of the TNF gene. *Curr. Dir. Autoimmun.* **11**, 27-60. doi:10.1159/000289196

Gleave Parson, M., Grimmett, J., Vance, J. K., Witt, M. R., Seman, B. G., Rawson, T. W., Lyda, L., Labuda, C., Jung, J.-Y., Bradford, S. D. et al. (2019). Murine myeloid-derived suppressor cells are a source of elevated levels of interleukin-27 in early life and compromise control of bacterial infection. *Immunol. Cell Biol.* **97**, 445-456. doi:10.1111/imcb.12224

Gupta, A. K., Joshi, M. B., Philippova, M., Erne, P., Hasler, P., Hahn, S. and Resink, T. J. (2010). Activated endothelial cells induce neutrophil extracellular traps and are susceptible to NETosis-mediated cell death. *FEBS Lett.* **584**, 3193-3197. doi:10.1016/j.febslet.2010.06.006

Hassani, M., Hellebrekers, P., Chen, N., van Aalst, C., Bongers, S., Hietbrink, F., Koenderman, L. and Vrisekoop, N. (2020). On the origin of low-density neutrophils. *J. Leukoc. Biol.* **107**, 809-818. doi:10.1002/JLB.5HR0120-459R

He, Y.-M., Li, X., Perego, M., Nefedova, Y., Kossenkov, A. V., Jensen, E. A., Kagan, V., Liu, Y.-F., Fu, S.-Y., Ye, Q.-J. et al. (2018). Transitory presence of myeloid-derived suppressor cells in neonates is critical for control of inflammation. *Nat. Med.* **24**, 224-231. doi:10.1038/nm.4467

Hirose, T., Hamaguchi, S., Matsumoto, N., Irisawa, T., Seki, M., Tasaki, O., Hosotsubo, H., Yamamoto, N., Yamamoto, K., Akeda, Y. et al. (2014). Presence of neutrophil extracellular traps and citrullinated histone H3 in the bloodstream of critically ill patients. *PLoS ONE* **9**, e111755. doi:10.1371/journal.pone.0111755

Holmgaard, R. B., Zamarin, D., Li, Y., Gasmi, B., Munn, D. H., Allison, J. P., Merghoub, T. and Wolchok, J. D. (2015). Tumor-expressed IDO recruits and activates MDSCs in a treg-dependent manner. *Cell Rep.* **13**, 412-424. doi:10.1016/j.celrep.2015.08.077

Hsu, B. E., Tabariès, S., Johnson, R. M., Andrzejewski, S., Senecal, J., Lehuédé, C., Annis, M. G., Ma, E. H., Völs, S., Ramsay, L. et al. (2019). Immature low-density neutrophils exhibit metabolic flexibility that facilitates breast cancer liver metastasis. *Cell Rep.* **27**, 3902-15.e6. doi:10.1016/j.celrep.2019.05.091

Huang, H.-C., Yu, H.-R., Huang, L.-T., Huang, H.-C., Chen, R.-F., Lin, I.-C., Ou, C.-Y., Hsu, T.-Y. and Yang, K. D. (2012). miRNA-125b regulates TNF-α production in CD14+ neonatal monocytes via post-transcriptional regulation. *J. Leukoc. Biol.* **92**, 171-182. doi:10.1189/jlb.1211593

Jablonska, J. and Granot, Z. (2017). Neutrophil, quo vadis? *J. Leukoc. Biol.* **102**, 685-688. doi:10.1189/jlb.3MR0117-015R

Janols, H., Bergenfelz, C., Allaoui, R., Larsson, A.-M., Rydén, L., Björnsson, S., Janciauskiene, S., Wullt, M., Bredberg, A. and Leandersson, K. (2014). A high frequency of MDSCs in sepsis patients, with the granulocytic subtype dominating in gram-positive cases. *J. Leukoc. Biol.* **96**, 685-693. doi:10.1189/jlb.5HI0214-074R

Knaul, J. K., Jörg, S., Oberbeck-Mueller, D., Heinemann, E., Scheuermann, L., Brinkmann, V., Mollenkopf, H.-J., Yeremeev, V., Kaufmann, S. H. E. and Dorhoi, A. (2014). Lung-residing myeloid-derived suppressors display dual functionality in murine pulmonary tuberculosis. *Am. J. Respir. Crit. Care. Med.* **190**, 1053-1066. doi:10.1164/rccm.201405-0828OC

Kontoyiannis, D., Pasparakis, M., Pizarro, T. T., Cominelli, F. and Kollias, G. (1999). Impaired on/off regulation of TNF biosynthesis in mice lacking TNF AU-rich elements: implications for joint and gut-associated immunopathologies. *Immunity* **10**, 387-398. doi:10.1016/S1074-7613(00)80038-2

Köstlin, N., Kugel, H., Spring, B., Leiber, A., Marmé, A., Henes, M., Rieber, N., Hartl, D., Poets, C. F. and Gille, C. (2014). Granulocytic myeloid derived suppressor cells expand in human pregnancy and modulate T-cell responses. *Eur. J. Immunol.* **44**, 2582-2591. doi:10.1002/eji.201344200

Kraft, J. D., Horzempa, J., Davis, C., Jung, J.-Y., Peña, M. M. O. and Robinson, C. M. (2013). Neonatal macrophages express elevated levels of interleukin-27 that oppose immune responses. *Immunology* **139**, 484-493. doi:10.1111/imm.12095

Kutcher, M. E., Xu, J., Vilardi, R. F., Ho, C., Esmon, C. T. and Cohen, M. J. (2012). Extracellular histone release in response to traumatic injury: implications for a compensatory role of activated protein C. *J. Trauma Acute Care Surg.* **73**, 1389-1394. doi:10.1097/TA.0b013e318270d595

La Manna, M. P., Orlando, V., Paraboschi, E. M., Tamburini, B., Di Carlo, P., Cascio, A., Asselta, R., Dieli, F. and Caccamo, N. (2019). Mycobacterium tuberculosis drives expansion of low-density neutrophils equipped with regulatory activities. *Front. Immunol.* **10**, 2761. doi:10.3389/fimmu.2019.02761

Leiber, A., Schwarz, J., Köstlin, N., Spring, B., Fehrenbach, B., Katava, N., Poets, C. F. and Gille, C. (2017). Neonatal myeloid derived suppressor cells show reduced apoptosis and immunosuppressive activity upon infection with Escherichia coli. *Eur. J. Immunol.* **47**, 1009-1021. doi:10.1002/eji.201646621

Lewis, H. D., Liddle, J., Coote, J. E., Atkinson, S. J., Barker, M. D., Bax, B. D., Bicker, K. L., Bingham, R. P., Campbell, M., Chen, Y. H. et al. (2015). Inhibition of PAD4 activity is sufficient to disrupt mouse and human NET formation. *Nat. Chem. Biol.* **11**, 189-191. doi:10.1038/nchembio.1735

Li, H., Han, Y., Guo, Q., Zhang, M. and Cao, X. (2009). Cancer-expanded myeloid-derived suppressor cells induce anergy of NK cells through membrane-bound TGF-β1. *J. Immunol.* **182**, 240-249. doi:10.4049/jimmunol.182.1.240

Li, P., Li, M., Lindberg, M. R., Kennett, M. J., Xiong, N. and Wang, Y. (2010). PAD4 is essential for antibacterial innate immunity mediated by neutrophil extracellular traps. *J. Exp. Med.* **207**, 1853-1862. doi:10.1084/jem.20100239

Miller-Ocuin, J. L., Liang, X., Boone, B. A., Doerfler, W. R., Singhi, A. D., Tang, D., Kang, R., Lotze, M. T. and Zeh, H. J.III (2019). DNA released from neutrophil extracellular traps (NETs) activates pancreatic stellate cells and enhances pancreatic tumor growth. *Oncoimmunology* **8**, e1605822. doi:10.1080/2162402X.2019.1605822

Moses, K. and Brandau, S. (2016). Human neutrophils: their role in cancer and relation to myeloid-derived suppressor cells. *Semin. Immunol.* **28**, 187-196. doi:10.1016/j.smim.2016.03.018

Murray, P. J. (2017). Macrophage Polarization. *Annu. Rev. Physiol.* **79**, 541-566. doi:10.1146/annurev-physiol-022516-034339

Neeli, I. and Radic, M. (2013). Opposition between PKC isoforms regulates histone deimination and neutrophil extracellular chromatin release. *Front Immunol* **4**, 38. doi:10.3389/fimmu.2013.00038

Nicolás-Ávila, J. A., Adrover, J. M. and Hidalgo, A. (2017). Neutrophils in homeostasis, immunity, and cancer. *Immunity* **46**, 15-28. doi:10.1016/j.immuni.2016.12.012

Ost, M., Singh, A., Peschel, A., Mehling, R., Rieber, N. and Hartl, D. (2016). Myeloid-derived suppressor cells in bacterial infections. *Front. Cell Infect. Microbiol.* **6**, 37. doi:10.3389/fcimb.2016.00037

Ostrand-Rosenberg, S., Sinha, P., Beury, D. W. and Clements, V. K. (2012). Cross-talk between myeloid-derived suppressor cells (MDSC), macrophages,

and dendritic cells enhances tumor-induced immune suppression. *Semin. Cancer Biol.* **22**, 275-281. doi:10.1016/j.semcancer.2012.01.011

Papayannopoulos, V. (2018). Neutrophil extracellular traps in immunity and disease. *Nat. Rev. Immunol.* **18**, 134-147. doi:10.1038/nri.2017.105

Park, M.-J., Lee, S.-H., Kim, E.-K., Lee, E.-J., Baek, J.-A., Park, S.-H., Kwok, S.-K. and Cho, M.-L. (2018). Interleukin-10 produced by myeloid-derived suppressor cells is critical for the induction of Tregs and attenuation of rheumatoid inflammation in mice. *Sci. Rep.* **8**, 3753. doi:10.1038/s41598-018-21856-2

Pillay, J., Tak, T., Kamp, V. M. and Koenderman, L. (2013). Immune suppression by neutrophils and granulocytic myeloid-derived suppressor cells: similarities and differences. *Cell. Mol. Life Sci.* **70**, 3813-3827. doi:10.1007/s00018-013-1286-4

Poe, S. L., Arora, M., Oriss, T. B., Yarlagadda, M., Isse, K., Khare, A., Levy, D. E., Lee, J. S., Mallampalli, R. K., Chan, Y. R. et al. (2013). STAT1-regulated lung MDSC-like cells produce IL-10 and efferocytose apoptotic neutrophils with relevance in resolution of bacterial pneumonia. *Mucosal. Immunol.* **6**, 189-199. doi:10.1038/mi.2012.62

Pugin, J., Heumann, I. D., Tomasz, A., Kravchenko, V. V., Akamatsu, Y., Nishijima, M., Glauser, M. P., Tobias, P. S. and Ulevitch, R. J. (1994). CD14 is a pattern recognition receptor. *Immunity* **1**, 509-516. doi:10.1016/1074-7613(94)90093-0

Rieber, N., Brand, A., Hector, A., Graepler-Mainka, U., Ost, M., Schäfer, I., Wecker, I., Neri, D., Wirth, A., Mays, L. et al. (2013a). Flagellin induces myeloid-derived suppressor cells: implications for Pseudomonas aeruginosa infection in cystic fibrosis lung disease. *J. Immunol.* **190**, 1276-1284. doi:10.4049/jimmunol.1202144

Rieber, N., Gille, C., Köstlin, N., Schäfer, I., Spring, B., Ost, M., Spieles, H., Kugel, H. A., Pfeiffer, M., Heininger, V. et al. (2013b). Neutrophilic myeloid-derived suppressor cells in cord blood modulate innate and adaptive immune responses. *Clin. Exp. Immunol.* **174**, 45-52. doi:10.1111/cei.12143

Rizzo, A., Campanile, D., Spedicato, M., Minoia, G. and Sciorsci, R. L. (2011). Update on anesthesia and the immune response in newborns delivered by cesarian section. *Immunopharmacol. Immunotoxicol.* **33**, 581-585. doi:10.3109/08923973.2010.549137

Rodriguez, P. C., Ernstoff, M. S., Hernandez, C., Atkins, M., Zabaleta, J., Sierra, R. and Ochoa, A. C. (2009). Arginase I-producing myeloid-derived suppressor cells in renal cell carcinoma are a subpopulation of activated granulocytes. *Cancer Res.* **69**, 1553-1560. doi:10.1158/0008-5472.CAN-08-1921

Rosales, C. (2018). Neutrophil: a cell with many roles in inflammation or several cell types? *Front. Physiol.* **9**, 113. doi:10.3389/fphys.2018.00113

Samraj, R. S., Zingarelli, B. and Wong, H. R. (2013). Role of biomarkers in sepsis care. *Shock* **40**, 358-365. doi:10.1097/SHK.0b013e3182a66bd6

Scapini, P., Marini, O., Tecchio, C. and Cassatella, M. A. (2016). Human neutrophils in the saga of cellular heterogeneity: insights and open questions. *Immunol. Rev.* **273**, 48-60. doi:10.1111/imr.12448

Sharma, A. A., Jen, R., Butler, A. and Lavoie, P. M. (2012). The developing human preterm neonatal immune system: a case for more research in this area. *Clin. Immunol.* **145**, 61-68. doi:10.1016/j.clim.2012.08.006

Simmons, D. L., Tan, S., Tenen, D. G., Nicholson-Weller, A. and Seed, B. (1989). Monocyte antigen CD14 is a phospholipid anchored membrane protein. *Blood* **73**, 284-289. doi:10.1182/blood.V73.1.284.284

Simon, A. K., Hollander, G. A. and McMichael, A. (2015). Evolution of the immune system in humans from infancy to old age. *Proc. Biol. Sci.* **282**, 20143085. doi:10.1098/rspb.2014.3085

Simonsen, K. A., Anderson-Berry, A. L., Delair, S. F. and Davies, H. D. (2014). Early-onset neonatal sepsis. *Clin. Microbiol. Rev.* **27**, 21-47. doi:10.1128/CMR.00031-13

Stoll, B. J., Hansen, N. I., Sanchez, P. J., Faix, R. G., Poindexter, B. B., Van Meurs, K. P., Bizzarro, M. J., Goldberg, R. N., Frantz, I. D., III, Hale, E. C. et al. (2011). Early onset neonatal sepsis: the burden of group B Streptococcal and E. coli disease continues. *Pediatrics* **127**, 817-826. doi:10.1542/peds.2010-2217

Ui Mhaonaigh, A., Coughlan, A. M., Dwivedi, A., Hartnett, J., Cabral, J., Moran, B., Brennan, K., Doyle, S. L., Hughes, K., Lucey, R. et al. (2019). Low density granulocytes in ANCA vasculitis are heterogenous and hypo-responsive to anti-myeloperoxidase antibodies. *Front. Immunol.* **10**, 2603. doi:10.3389/fimmu.2019.02603

van der Poll, T., van de Veerdonk, F. L., Scicluna, B. P. and Netea, M. G. (2017). The immunopathology of sepsis and potential therapeutic targets. *Nat. Rev. Immunol.* **17**, 407-420. doi:10.1038/nri.2017.36

Villanueva, E., Yalavarthi, S., Berthier, C. C., Hodgin, J. B., Khandpur, R., Lin, A. M., Rubin, C. J., Zhao, W., Olsen, S. H., Klinker, M. et al. (2011). Netting neutrophils induce endothelial damage, infiltrate tissues, and expose immunostimulatory molecules in systemic lupus erythematosus. *J. Immunol.* **187**, 538-552. doi:10.4049/jimmunol.1100450

Wang, Y., Li, M., Stadler, S., Correll, S., Li, P., Wang, D., Hayama, R., Leonelli, L., Han, H., Grigoryev, S. A. et al. (2009). Histone hypercitrullination mediates chromatin decondensation and neutrophil extracellular trap formation. *J. Cell Biol.* **184**, 205-213. doi:10.1083/jcb.200806072

Weston, E. J., Pondo, T., Lewis, M. M., Martell-Cleary, P., Morin, C., Jewell, B., Daily, P., Apostol, M., Petit, S., Farley, M. et al. (2011). The burden of invasive early-onset neonatal sepsis in the United States, 2005-2008. *Pediatr. Infect. Dis. J.* **30**, 937-941. doi:10.1097/INF.0b013e318223bad2

Wildhagen, K. C. A. A., Garcia de Frutos, P., Reutelingsperger, C. P., Schrijver, R., Aresté, C., Ortega-Gómez, A., Deckers, N. M., Hemker, H. C., Soehnlein, O. and Nicolaes, G. A. (2014). Nonanticoagulant heparin prevents histone-mediated cytotoxicity in vitro and improves survival in sepsis. *Blood* **123**, 1098-1101. doi:10.1182/blood-2013-07-514984

Wirestam, L., Arve, S., Linge, P. and Bengtsson, A. A. (2019). Neutrophils-important communicators in systemic lupus Erythematosus and Antiphospholipid Syndrome. *Front. Immunol.* **10**, 2734. doi:10.3389/fimmu.2019.02734

Wright, H. L., Makki, F. A., Moots, R. J. and Edwards, S. W. (2017). Low-density granulocytes: functionally distinct, immature neutrophils in rheumatoid arthritis with altered properties and defective TNF signalling. *J. Leukoc. Biol.* **101**, 599-611. doi:10.1189/jlb.5A0116-022R

Xu, J., Zhang, X., Pelayo, R., Monestier, M., Ammollo, C. T., Semeraro, F., Taylor, F. B., Esmon, N. L., Lupu, F. and Esmon, C. T. (2009). Extracellular histones are major mediators of death in sepsis. *Nat. Med.* **15**, 1318-1321. doi:10.1038/nm.2053

Yao, Y., Xie, Y. and Kim, K. S. (2006). Genomic comparison of Escherichia coli K1 strains isolated from the cerebrospinal fluid of patients with meningitis. *Infect. Immun.* **74**, 2196-2206. doi:10.1128/IAI.74.4.2196-2206.2006

Youn, J.-I., Collazo, M., Shalova, I. N., Biswas, S. K. and Gabrilovich, D. I. (2012). Characterization of the nature of granulocytic myeloid-derived suppressor cells in tumor-bearing mice. *J. Leukoc. Biol.* **91**, 167-181. doi:10.1189/jlb.0311177

Young, M. R., Newby, M. and Wepsic, H. T. (1987). Hematopoiesis and suppressor bone marrow cells in mice bearing large metastatic Lewis lung carcinoma tumors. *Cancer Res.* **47**, 100-105.